Research Note

This is an extended version of the paper presented in SEE7 conference, peer-reviewed again and approved by the JSEE editorial board.

Cyclic Analysis of RC Shear Walls, Considering Bar-Concrete Interaction

Hamze Zarei Chargoad[1], Seyed Shaker Hashemi[2*], and Mohammad Vaghefi[3]

1. M.Sc. Graduate, Civil Engineering Department, Persian Gulf University, Bushehr, Iran
2. Assistant Professor, Civil Engineering Department, Persian Gulf University, Bushehr, Iran,
* Corresponding Author; email: sh.hashemi@pgu.ac.ir
3. Associate Professor, Civil Engineering Department, Persian Gulf University, Bushehr, Iran

Received: 02/09/2015
Accepted: 16/12/2015

ABSTRACT

In this paper, the nonlinear behavior of reinforced concrete shear wall with consideration of bond-slip effect between the bars and surrounding concrete is investigated. Bar and concrete stress-strain relations, the bond stress-slip relation and the shear stress-strain relation as well as their cyclic behavior including the strength degradation and stiffness degradation are adopted known specifications. In the modeling, shear wall is divided into two types of joint element and RC element. In RC element, the effect of shear deformation is considered and based on Timoshenko beam theory the effect of shear has been considered during the calculation. A numerical model based on the fiber method is used for nonlinear analysis of reinforced concrete shear wall. Separate degrees of freedom are used for the steel and concrete parts to allow for the difference in displacement between the reinforcing bars and the surrounding concrete. The effect of bond-slip has been considered in the formulation of an RC element by replacing the perfect bond assumption from the fiber analysis method. The effects of embedded length and pull-out force on the seismic behavior of a reinforced concrete shear wall were investigated. The reliability of the method has been assessed through a comparison of numerical and experimental results for a variety of specimens tested under cyclic loading. A good agreement between experimental and analytical results is obtained for both cases of strength and stiffness during the analysis.

Keywords:
Nonlinear analysis; Bond-slip effect; Shear deformation; Reinforced concrete shear wall

1. Introduction

Many analytical models have been devised for nonlinear analysis of reinforced concrete shear wall. The analytical model can be separated into two groups: macroscopic models and microscopic models. The macroscopic models are based on representing the overall behavior of the RC shear wall, such as the wall deformations, strength, and energy dissipation capacity. Various macroscopic models have been proposed to predict the nonlinear response of RC structural walls. The first method used to analyze the shear walls, is the equivalent beam-column element that is still widely used to study walls behavior. In this model, the wall is replaced by a column with walls equivalent cross section properties. The limitation of this approach is that it assumes rotations occur around the central axis of the wall. Therefore, it ignores the change in neutral axis of the wall section and interactions with members of the frame, which are connected to the wall. Besides, due to neglecting the progressive opening of the cracks associated with shifting of the neutral axis, rotation and displacement in this method are less than reality. These limitations led to use multiple elements method of the vertical component [1]. In addition to removing restrictions of shifting neutral axis, these procedures express more accurately the tensile hardening of concrete, progressive opening and closing of cracks and shear nonlinear behavior of concrete confinement. Based on results of a full-scale test of a seven-story RC frame-wall building, three- vertical-line-element model was proposed by Kabeyasawa et al [2]. The model, account the experimentally observed behavior, which equivalent beam-column model could not be describe it. In this model, the wall member was modeled as three vertical line elements with infinitely rigid beams at the top and bottom levels. This model modified by Vulcano and Bertero [3], and consists of replacing the axial spring of the boundary element with two axial element connected in series. Vulcano et al [4] proposed the multi component in parallel model to predict the flexural and shear behavior of the wall, but their responses were not coupled. This component represents the cracked concrete and steel reinforcement behavior. Fischinger et al [5] presented simple hysteretic rules for vertical and horizontal springs in multiple-vertical-line element model, and Fischinger et al [6] have shown that the modified of multiple-vertical-line element model was well suited for modeling coupled wall response. In order to consider the flexure-shear interaction in the reinforced concrete structural wall, a new model was presented by Massone and Wallace [7] that concluded overestimated the flexural deformations and low estimated the shear deformations. The other macroscopic modeling approaches that can be noted are truss model, two-component beam-column element, one-component beam-column element, multiple spring model and multi-axial spring model [8]. Development of this modeling approach has led to the layer element in which the cross section of the wall is divided into the certain number of elements. Most of these methods assume that the bond between the reinforcing bars and the surrounding concrete is perfect and the slip is neglected. However, this assumption is not very appropriate and realistic, and causes a considerable difference between numerical and experimental results. The most promising model for the nonlinear analysis of reinforced concrete elements is, presently, fiber section model. The fiber model, basically, adopts the perfect bond assumption. This assumption causes a considerable difference between experimental and analytical responses of the reinforced concrete shear wall in many cases. Monti and Spacone [9] calculated the bond slip effect of the reinforcement bars in the fiber section model. This model was used by Kotronis et al [10] to simulate nonlinear behavior of reinforced concrete walls subjected to earthquake ground motion. Belmouden and Lestuzzi [11] use this model to predict nonlinear reversed cyclic behavior of reinforced concrete shear walls based on the tests conducted. Assuming a linear shear deformation, the complexity of the simulation boundary conditions, and ignoring the bond slip effect were the limitations of this model. In this paper, a numerical model based on the fiber method is used for nonlinear analysis of reinforced concrete shear wall. The theory of numerical calculation is similar to fiber method; however, the perfect bond assumption between the bars and surrounding concrete has been removed. Separate degrees of freedom are used for the steel and concrete parts in nonlinear modelling of the reinforced concrete elements [12].

2. Nonlinear Modelling of RC Shear Wall with Bond-Slip Effect

The theory in this research is the development of fiber model. In this model, the member is divided longitudinally into several segments, and each segment is composed of parallel layers. Some layers would represent the concrete material and other layers would represent the steel material. Behavior of concrete and steel are separately defined, but the interaction between them is not considered. For the purpose of nonlinear analysis of RC shear wall and investigation of the bond-slip effect, two types of RC and joint elements are modelled as Figure (1). The bond-slip effect has been considered in the formulation of reinforced concrete elements and joint element. The effect of bond-slip has been considered in the formulation of a reinforced concrete element by replacing the perfect bond assumption from the fiber analysis method. Joint elements are formulated upon major behavior including the pull-out of embedded longitudinal bars [13-14].

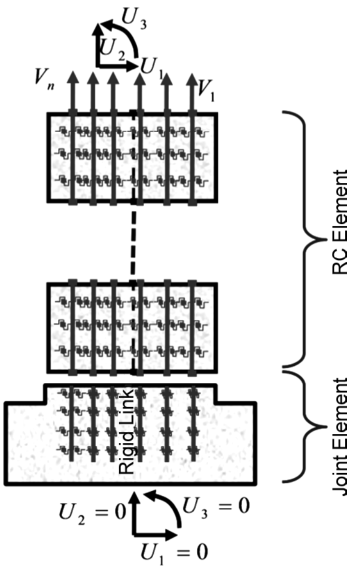

Figure 1. Numerical modeling of an RC shear wall.

For modeling an RC Element based on research carried out by Limkatanyu and Spacone [15] in the fiber model, the slip effect between concrete and bar is implemented without ignoring the compatibility of the strain between the concrete and bar. In this element, the effect of shear deformation is considered and based on Timoshenko beam theory, the effect of shear has been considered in calculation. Timoshenko beam theory assumes that the cross section remains plane after deformation, but the Euler-Bernoulli beam theory neglects shear deformations by assuming that plane sections remain plane and perpendicular to the beam axis during bending. As a result, shear strains and stresses are removed from the theory. However, the Timoshenko beam theory is based on the shear deformation. It is assumed that the cross section remains plane and is not necessarily perpendicular to the longitudinal axis after deformation because of shear deformation. In Figure (2), the comparison between Euler Bernoulli and Timoshenko beam theory is presented [16].

According to Figure (2), if the section a-b change into a'- b' after the internal deformation, in Euler Bernoulli beam theory this surface is remain perpendicular to the main axis of element, but in Timoshenko beam theory these conditions are not established.

The free body diagram of an infinitesimal segment, dx, of RCE is shown in Figure (3). Each RCE is introduced as a combination of one 2-node concrete element and n number of 2-node bars with bond interfaces. Slippage is allowed to occur, because the nodal degrees of freedom of the concrete element and that of the bars are different. Based on small deformation assumptions, all equilibrium conditions are considered. Considering axial equilibrium in the concrete element and steel bars, as well as the vertical and moment equilibriums in segment *dx*, leads to a matrix form of equations given by Eq. (1):

$$\partial_B^T \mathbf{D}_B(x) - \partial_b^T \mathbf{D}_b(x) - \mathbf{p}(x) = 0 \qquad (1)$$

where: $\mathbf{D}_B(x) = \{\overline{\mathbf{D}}(x) : \overline{\overline{\mathbf{D}}}(x)\}^T$ is the vector of RCE section forces. $\overline{\mathbf{D}}(x) : \{N(x)\ V_y(x)\ M_y(x)\}^T$ is the vector of concrete element section forces. $\mathbf{D}_b(x) : \{D_{b1}(x)\ \ldots\ D_{bn}(x)\}^T$ is the vector of bar axial forces. This vector has n rows. $\mathbf{P}(x)$: $\{0\ \ p_y\ \ 0\ \ 0\ \ \ldots\ \ 0\}^T$ is the vector of bond section forces. p_y is the vector RCE force vector. n is the number of longitudinal bars in the cross section. p_y is the value of external load. ∂_B, ∂_b are differential operators that are given in Eq. (2).

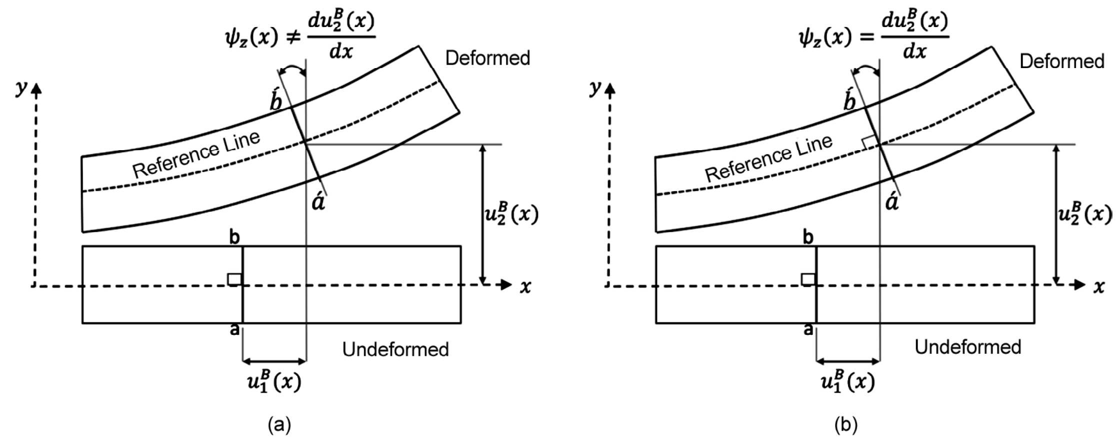

Figure 2. Internal deformations. Comparison between (a) Timoshenko beam theory and (b) Euler Bernoulli beam theory.

$$\partial_B = \begin{bmatrix} \bar{\partial}_B & 0 \\ 0 & \bar{\bar{\partial}}_B \end{bmatrix}, \quad \bar{\partial}_B = \begin{bmatrix} \frac{d}{dx} & 0 & 0 \\ 0 & \frac{d}{dx} & -1 \\ 0 & 0 & \frac{d}{dx} \end{bmatrix},$$

$$\bar{\bar{\partial}}_B = \begin{bmatrix} \frac{d}{dx} & 0 & \dots & 0 \\ 0 & \frac{d}{dx} & \dots & 0 \\ \dots & \dots & \dots & \dots \\ 0 & 0 & \dots & \frac{d}{dx} \end{bmatrix} \tag{2}$$

$$\partial_b = \begin{bmatrix} -1 & 0 & y_1 & 1 & 0 & \dots & 0 \\ -1 & 0 & y_2 & 0 & 1 & \dots & 0 \\ \dots & \dots & \dots & \dots & \dots & \dots & 0 \\ -1 & 0 & y_n & 0 & 0 & \dots & 1 \end{bmatrix}_{n^*(n+3)}$$

y_n is the distance of bar n from the section reference axis (Figure 3). The RCE section deformation vector conjugate of $\mathbf{D}_B(x)$ is $\mathbf{d}_B(x):\{\bar{\mathbf{d}}_B(x):\bar{\bar{\mathbf{d}}}_B(x)\}^T$ in which $\bar{\mathbf{d}}(x) = \{\varepsilon_B(x) \quad \gamma_y(x) \quad \kappa_B(x)\}^T$ contains concrete element section deformations and $\bar{\bar{\mathbf{d}}}(x) = \{\varepsilon_1(x) \quad \dots \quad \varepsilon_n(x)\}^T$ contains the axial strain of the bars. The displacement vector in the cross section of RCE is defined as $\mathbf{u}(x):\{\bar{\mathbf{u}}(x):\bar{\bar{\mathbf{u}}}_B(x)\}^T$, in which $\bar{\mathbf{u}}(x) = \{u_B^1(x) \quad u_B^2(x) \quad \Psi_z(x)\}^T$, contains concrete element axial and transversal displacements, respectively, and $\bar{\bar{\mathbf{u}}}(x) = \{u_1(x) \quad \dots \quad u_n(x)\}^T$ contains the axial displacements of the bars. From a small deformation assumption, the element deformations are related to the element displacements through the following relation:

$$\mathbf{d}_B(x) = \partial_B \mathbf{u}(x) \tag{3}$$

The slips of bars in the section of RC element are determined by the following relation between the bar and concrete element displacements:

$$u_{bi}(x) = v_i(x) - u_1^B(x) + y_i \psi_z(x) \tag{4}$$

where, $v_i(x)$ is bar axial displacement and $u_1^B(x)$ is displacements in axial of concrete element. By introducing the bond deformation vector as $\mathbf{d}_b(x) = \{u_{b1}(x) \quad \dots \quad u_{bn}(x)\}^T$, Eq. (4) can be written in the following matrix form:

$$\mathbf{d}_b(x) = \partial_b \mathbf{u}(x) \tag{5}$$

The weak form of displacement based finite element formulation is determined through the principle of stationary potential energy. More details can be found in [13] (Figure 4).

A joint element is used as the footing connection of the RC shear wall. In this element, the effect of pull-out is considered as the relative displacement between the steel bar and surrounding concrete and bond stress is referred to as the shear stress acting parallel to an embedded steel bar on the contact surface between reinforcing bar and concrete.

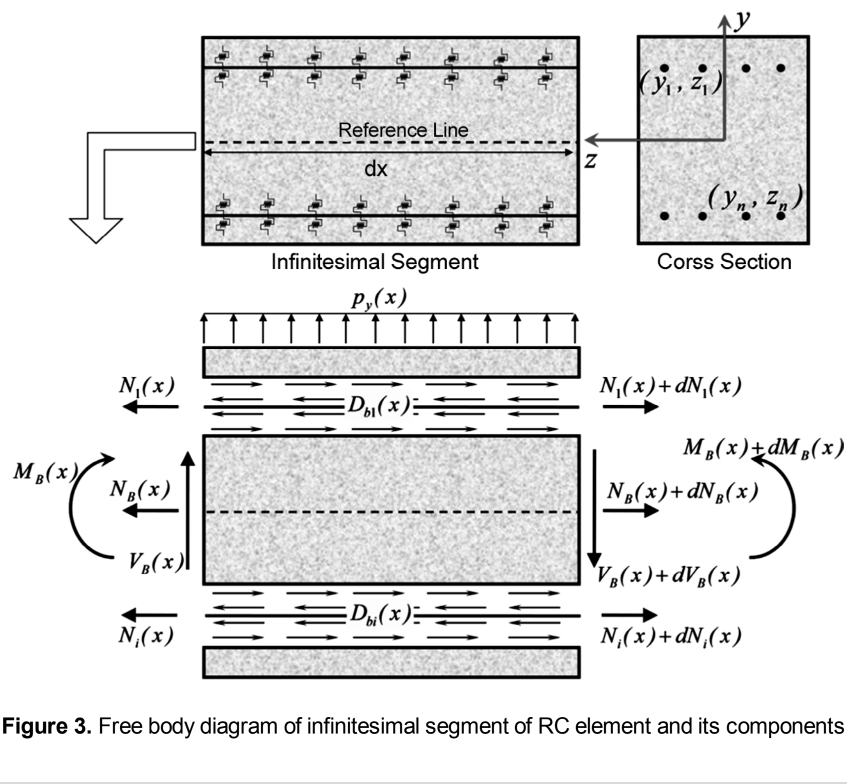

Figure 3. Free body diagram of infinitesimal segment of RC element and its components.

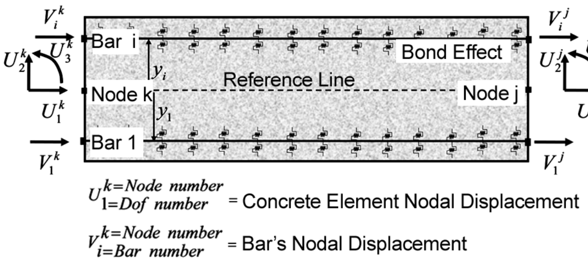

Figure 4. Reinforced concrete element..

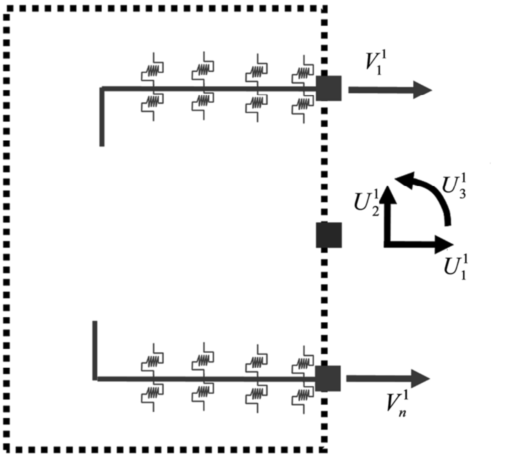

Figure 5. Numerical modelling of the bar's pull-out.

Referring to Figure (5), the slippage of the bars can be defined in the form of Eq. (6) if the nodal displacement vector related to pull-out behavior is defined as $\mathbf{U}_{PM}(x) = [U_1 \;\; U_2 \;\; U_3 \;\; V_1 \;\; V_n]^T$.

$$\mathbf{slip} = \begin{bmatrix} d_{b1} \\ \dots \\ d_{bi} \\ \dots \\ d_{bn} \end{bmatrix} = \begin{bmatrix} -1 & 0 & y_1 & 0 & \dots & 0 \\ -1 & 0 & y_2 & 0 & \dots & 0 \\ \dots & \dots & \dots & \dots & \dots & \dots \\ -1 & 0 & y_n & 0 & 0 & 1 \end{bmatrix}_{n^*(n+3)} \times \quad (6)$$

$$\mathbf{U}_{PM} = \mathbf{A}_{PM} \times \mathbf{U}_{PM}$$

In this equation, y_n is the distance of the n^{th} bar from the reference line. The relationship between the pull-out force and the slip for embedded bars derives from the bond stress-slip relationship related to pull-out behavior, embedded length of the bar, conditions at the end of the bar and perimeter of the bar cross section. A computer program created in MATLAB software was used by the authors [17].

3. Material Behaviors

3.1. Concrete cyclic Stress-Strain Relation

The monotonic envelope curve for confined concrete, introduced by Park et al [18] and later extended by Scott et al [19], is adopted for the compression region because of its simplicity and computational efficiency. Besides, it is assumed that concrete behavior is linearly elastic in the tension region before the tensile strength and, beyond that, the tensile stress decreases linearly with increasing tensile strain. Ultimate state of tension behavior is assumed to occur when tensile strain exceeds the value given in Eq. (7).

$$\varepsilon_{ut} = 2 \times \left(\frac{G_f}{f_t} \right) \times \ln\left(\frac{3}{L} \right) / (3 - L) \quad (7)$$

where L denotes the element length in mm and G_f is the fracture energy that is dissipated in the formation of cracks of unit length per unit thickness and is considered as a material property. f_t is concrete tensile strength. For normal strength concrete, the value of G_f / f_t is in the range of 0.005-0.01 [20]. In this research, the average value of 0.0075 is assumed for G_f / f_t. The rules suggested by Karsan and Jirsa [21] are adopted for the hysteresis behavior of the concrete stress-strain relation in the compression region. In addition, the unloading-reloading branches that always pass the origin, regardless of the loading history, are assumed in the tension region, because the application of the introduced numerical model is limited to *RC* frame structures [22].

3.2. Cyclic Stress-Strain Relation of Steel Bars

The Giuffre-Menegoto-Pinto model is adopted to represent the stress-strain relationship of steel bars. This model was initially proposed by Giuffre and Pinto [23] and later used by Menegoto and Pinto [24]. This model is modified by Filippou et al [25] to include isotropic strain hardening. The model agrees very well with experimental results from cyclic tests of reinforcing steel bars. The stress-strain relation can be expressed be Eq. (8).

$$\sigma^* = b\varepsilon^* + \frac{(1-b)\varepsilon^*}{(1+\varepsilon^{*R})^{1/R}} \quad (8)$$

where $\varepsilon^* = (\varepsilon - \varepsilon_r)/(\varepsilon_0 - \varepsilon_r)$, $\sigma^* = (\sigma - \sigma_r)/(\sigma_0 - \sigma_r)$. Eq. (8) expresses a curved transition from a straight line with slope E_0 to another straight line with slope E_1.

3.3. Cyclic Bond Stress-Slip Relation

Bond stress is referred to as the shear stress acting parallel to an embedded steel bar on the contact surface between the reinforcing bar and the concrete. Bond slip is defined as the relative displacement between the steel bar and the concrete. The adopted model to represent the bond slip effect between bars and concrete is proposed by Eligehausen et al [26]. In this model, the effect of many variables, such as the spacing and height of the lugs on the steel bar, the compressive strength of the concrete, the thickness of the concrete cover, the steel bar diameter, and the end bar hooks, are considered. More details about unloading and reloading branches and bond strength degradation related to this model are given in [27].

3.4. Cyclic Shear Stress-Strain Relation

The adopted model to represent the shear stress-strain of a joint is the one proposed by Anderson et al [28]. This model replicates cyclic degradation in strength, stiffness (modulus) state of behavior (Figure 6).

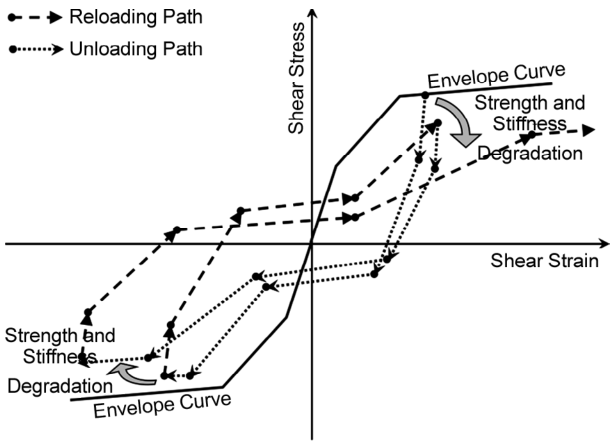

Figure 6. Cyclic shear stress - strain relation [28].

4. Numerical Investigation

For a reinforced concrete shear wall with geometric specifications according to Figure (7) and details provided under the name of Specimens 1 to 2 in the Table (1), numerical validation has been done. These specimens are two shear walls under uni-axial bending and constant axial load with magnitude of 630 kN for Specimens 1 and 1420 kN for Specimen 2. Lateral cyclic displacement was imposed at the free end. It was tested by Dazio et al [29].

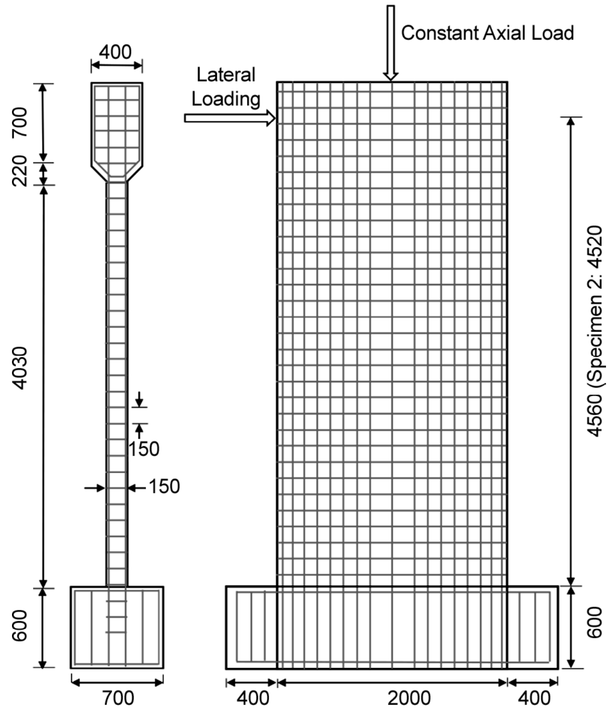

Figure 7. Geometry of the tested shear wall (all dimensions in mm) [29].

Table 1. Details of investigated specimens [29].

	Specimen 1	Specimen 2
Main Bars	12Φ12mm and 22Φ8mm	12Φ12mm and 22Φ8mm
Stirrups	Φ6@150mm and (Φ6 and Φ4.2) @75mm	Φ6@150mm and (Φ6 and Φ4.2) @50mm
f_y of Main Bars (MPa)	601 for Φ12 and 569.2 for Φ8	576 for Φ12 and 583.7 for Φ8
f_y of Stirrups Bars (MPa)	489	518.9
f_y of Closed Ties and S- Shaped Ties (MPa)	489 for Φ6 and 562.2 for Φ4.2	518.9 for Φ6 and 562.2 for Φ4.2
f_c (MPa)	39.2	45.6
Concrete Cover (mm)	30	30

The dimensions of the section of specimens, size and arrangement of the longitudinal bars are the same in both specimens, but the strength of concrete, size and arrangement of the transverse bars are different. The cross section of specimens is 2.00 m long and 0.15 m wide. Location of applying lateral load is 4.56 m above the foundation for Specimen 1 and 4.52 m for Specimen 2. The Cross sections of specimens are shown in Figure (8).

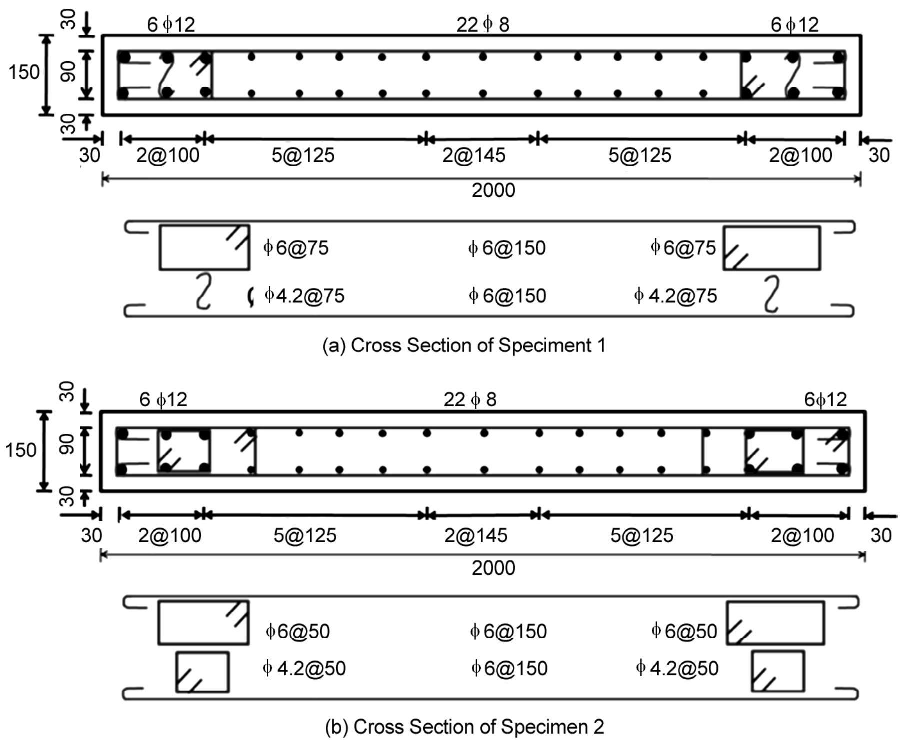

Figure 8. Reinforcement and section geometry of specimens (all dimensions in mm) [29].

In numerical modeling, the wall is subdivided into enough number of shorter elements, because the formulation is displacement based, the response depends on element size and the length of elements is needed to be short enough. As a simple suggestion, the length of the RC elements can be selected smaller than or equal to the average crack spacing in the wall [30]. In these cases, convergence of the calculated responses will be achieved in the numerical process. The minimum required embedded length is satisfied in all Specimens in order to prevent pull-out of the bars from the footing connection and affect the results. For nonlinear solving of this model, a Newton-Raphson method that involved controlling displacement was used. Figures (9) and (10) show the analytical and experimental load-displacement responses for Specimens 1 and 2, respectively. Results show good accordance for strength, stiffness, and their changes during cyclic loading.

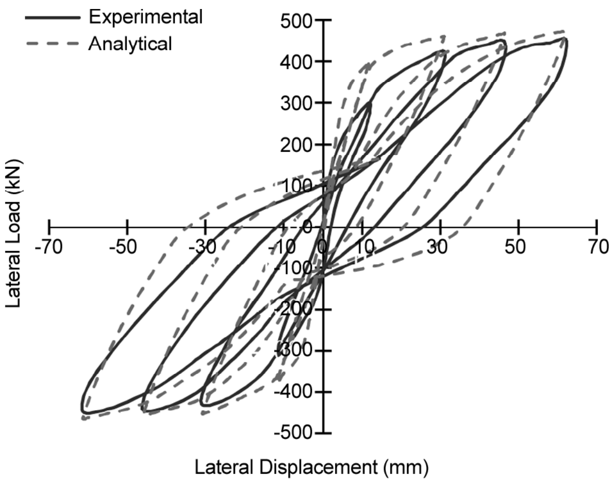

Figure 9. Experimental and analytical cyclic load-displacement response for Specimen1.

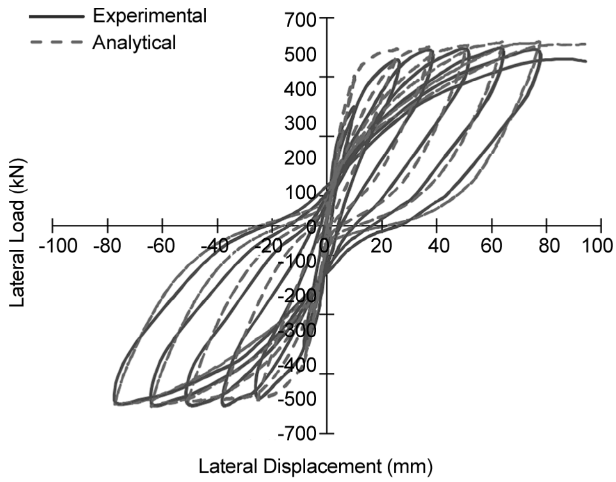

Figure 10. Experimental and analytical cyclic load- displacement response for Specimen2.

5. Conclusions

In this research, a numerical model based on the fiber model is introduced for nonlinear cyclic analysis of two-dimensional RC shear wall. The advantage of the proposed analytical procedure is that it takes bond-slip, pull-out effects and shears deformation into account. Formulation is displacement-based and shape functions are used in order to express internal displacements in terms of nodal displacement. To model each wall, two types of joint element and *RC* element are used. The effect of bond-slip is considered in the formulation of *RC* element by replacing the perfect bond assumption from the fiber analysis method. Accuracy of the analytical method proposed in this study is very good due to considering the bond slip effect and also the effect of shear deformation in the calculation.

The reliability of the method is assessed through a variety of tested specimens under cyclic loading and good agreement between experimental and numerical results is obtained for both cases of strength and stiffness during the analysis. The results show that the presence or absence of bond slip effect and shear deformation in numerical analysis of shear walls causes considerable difference in the responses parameters such as the ultimate capacity and stiffness.

References

1. Orakcal, K., Massone, L.M., and Wallace, J.W. (2006) *Analytical Modelling of Reinforced Concrete Walls for Predicting Flexural and Coupled Shear-Flexural Responses*. Department of Civil and Environmental Engineering University of California, Los Angeles PEER Report.

2. Kabeyasawa, T., Shiohara, H., Otani, S., and Aoyama, H. (1983) Analysis of the full-scale seven-story reinforced concrete test structure. *Journal of the Faculty of Engineering, University of Tokyo*, **37**(2), 431-478.

3. Vulcano, A. and Bertero, V.V. (1986) Nonlinear analysis of RC structural walls. *Proceedings of 8th European Conference on Earthquake Engineering*, V.3. Lisbon, Portugal, 6.5/1-6.5/8.

4. Vulcano, A., Bertero, V.V., and Colotti, V. (1988) Analytical modeling of RC structural walls. *Proceedings of 9th World Conference on Earthquake Engineering*, V. 6, Tokyo-Kyoto, Japan, 41-46.

5. Fischinger, M., Vidic, T., Selih, J., Fajfar, P., Zhang, H.Y., and Damjanic, F.B. (1990) 'Validation of a macroscopic model for cyclic response prediction of RC walls'. In: *Bicanic, N. B. and Mang, H. (eds.), Computer Aided Analysis and Design of Concrete Structures*. V. 2, Pineridge Press, Swansea, 1131-1142.

6. Fischinger, M., Vidic, T. and Fajfar, P. (1992) 'Nonlinear Seismic Analysis of Structural Walls Using the Multiple-Vertical-Line-Element Model'. In: *Nonlinear Seismic Analysis of RC Buildings*, H. Krawinkler and P. Fajfar (eds.), Elsevier Science Publishers Ltd, London and New York, 191-202.

7. Massone, L.M. and Wallace, J.W. (2004) Load-deformation responses of slender reinforced concrete walls. *ACI Structural Journal*, **101**(1), 103-113.

8. Galal, K. and El-Sokkary, H. (2008) Advancement in modelling of RC shear walls. *Proceedings of 14th World Conference on Earthquake Engineering*, Beijing, China.

9. Monti, G. and Spacone, E. (2000) Reinforced concrete fiber beam element with bond-slip. *Journal of Structural Engineering*, ASCE, **126**(6), 654-661.

10. Kotronis, P., Ragueneau, F., and Mazars, J.A. (2005) Simplified model strategy for R/C walls satisfying PS92 and EC8 design. *Journal of Engineering Structures*, **27**(8), 1197-1208.

11. Belmouden, Y. and Lestuzzi, P. (2007) Analytical model for predicting nonlinear reversed cyclic behavior of reinforced concrete structural walls. *Journal of Engineering Structures*, **29**(7), 1263-1276.

12. Hashemi, S.SH. and Vaghefi, M. (2012) Investigation of the effect of a bar's inadequate embedded length on the P-M interaction curve of reinforced concrete columns with rectangular sections. *Turkish Journal of Engineering and*

Environmental Sciences, 36, 109-119.

13. Hashemi, S.SH., Tasnimi, A.A., and Soltani, M. (2009) Nonlinear cyclic analysis of reinforced concrete frames, utilizing new joint element. *Journal of Scientia Iranica, Transaction A*, **16**(6), 4901-501.

14. Hashemi, S.SH., Tasnimi, A.A., and Soltani, M. (2011) Nonlinear analysis of three dimensional reinforced concrete frames, considering bar-concrete interaction. *Journal of Faculty of Engineering (JFE)*, ISSN: 0803-1026, **45**(2), 141-154 (in Persian).

15. Limkatanyu, S. and Spacone, E. (2002) Reinforced concrete frame element with bond interfaces. Part I: displacement-based, force--based, and mixed formulations. *Journal of Structural Engineering*, ASCE, **128**(3), 346-355.

16. Kwon, Y.W. and Bang, H. (2000) *The Finite Element Method Using MATLAB*. Second edition, CRC press LCC publisher, USA.

17. MathWorks, MATLAB (2010) *The Language of Technical Computing*. Version 7.11.0. (R2010a).

18. Park, R., Kent, D.C., and Sampton, R.A. (1972) Reinforced concrete members with cyclic loading. *Journal of the Structural Division*, ASCE, **98**(7), 1341-1360.

19. Scott, B.D., Park, R., and Priestley, M.J.N. (1982) Stress-strain behavior of concrete confined by overlapping hoops at low and high strain rates. *ACI Journal*, **79**(1), 13-27.

20. Welch, G.B. and Haisman, B. (1969) *Fracture Toughness Measurements of Concrete*. Report No. R42, Sydney: University of New South Wales.

21. Karsan, I.D. and Jirsa, J.O. (1969) Behavior of concrete under compressive loading. *Journal of Structural Division*, ASCE, **95**(12), 2543-2563.

22. Kwak, H.G. and Kim, S.P. (2002) Cyclic moment-curvature relation of an RC beam. *Magazine of Concrete Research*, **54**(6), 435-447.

23. Giuffre, A. and Pinto, P.E. (1970) *Il comportamento del cemento armato per sollecitazzioni cicliche di forte intensita*. Giornale del Genio Civile, Maggio, (in Italian).

24. Menegoto, M. and Pinto, P. (1973) Method of analysis for cyclically loaded RC plane frames including changes in geometry and non-elastic behavior of elements under combined normal force and bending. *Symp. Resistance and Ultimate Deformability of Structures Acted on by Well Defined Repeated Loads*, IABSE Reports, Vol. 13, Lisbon.

25. Filippou, F.C., Popov, E. and Bertero, V. (1983) *Effect of Bond Deterioration on Hysteretic Behavior of Reinforced Concrete Joints*. Report No. EERC 83-19, Earthquake Engineering Research Center, University of California, Berkeley.

26. Eligehausen, R., Popov, E., and Bertero, V. (1983) *Local Bond Stress-Slip Relationship of Deformed Bars under Generalized Excitations*. Report UCB/EERC-83/23, Earthquake Engineering Center, University of California, Berkeley.

27. Gan, Y. (2000) *Bond Stress and Slip Modeling in Nonlinear Finite Element Analysis of Reinforced Concrete Structures*. A Thesis Submitted for Degree of Master of Applied Science Graduate, Department of Civil Engineering, University of Toronto.

28. Anderson, M., Lehman, D. and Stanton, J. (2008) A cyclic shear stress-strain model for joints without transverse reinforcement. *Engineering Structures*, **30**, 941-954.

29. Dazio, A., Beyer, K., and Bachmann H. (2009) Quasi-static cyclic tests and plastic hinge analysis of RC structural walls. *Engineering Structures*, **31**, 1556-1571.

30. Comite Euro International du Beton (1978) CEB-FIP Model Code for Concrete Structures. Paris.